since 1961

Baltica

BALTICA Volume 39 Number 2 December 2026: 131–147
https://doi.org/10.5200/baltica.2026.2.1

Research article

Seismic absorption coefficients and soil dynamic characteristics: implications for seismic hazard in Erzurum Basin, Türkiye

Ufuk Aydin, Caglar Ozer, Erdem Bayrak*

Aydin, U., Ozer, C., Bayrak, E. 2026. Seismic absorption coefficients and soil dynamic characteristics: implications for seismic hazard in Erzurum Basin, Türkiye. *Baltica 39 (2)* 131–147. Vilnius. ISSN 1648-858X.
Manuscript submitted 9 October 2025 / Accepted 25 May 2026 / Available online 29 June 2026

Abstract. In this study, the seismic absorption coefficients and nine seismic sub-regions for seismic hazard that may affect the Erzurum city centre were determined. Recurrence periods and the probabilities of occurrence of earthquakes above a specified magnitude threshold within a given time window were quantitatively estimated for each sub-region. The relationship between the seismic absorption coefficients and the probability of major earthquakes was analyzed, and the potential effects of these seismogenic structures on the Erzurum city centre were evaluated. Following the seismic hazard-based regionalization, the Erzurum city centre was further subdivided into eight sub-regions. A total of 24 microtremor measurements (three per sub-region) were conducted to characterize the dynamic soil properties within these sub-regions using passive seismic data. The seismic absorption coefficients, magnitude distributions and variations in dynamic soil characteristics of Erzurum were assessed regionally. Seismic hazard analyses conducted for nine different areas particularly highlighted the potential of major fault zones around Erzincan, Varto, and Bingol, specifically the North Anatolian Fault Zone and East Anatolian Fault Zone, to generate high-magnitude earthquakes. Seismic attenuation analyses revealed an average absorption coefficient of 0.02475 across the region, with values lower in the eastern and western sections and higher in the northern and southern sections. These results indicate that seismic energy distribution in the region has a heterogeneous structure and that geological features play a decisive role in this process. Microtremor measurements showed that soil amplification factor in the Dadaskent region reached significant values below 1 Hz, indicating that this area is critical in terms of earthquake-soil-structure interaction. Consequently, the combined effects of high amplification and regionally variable attenuation characteristics imply an increased seismic hazard potential for the Erzurum city centre, particularly in zones with unfavourable local site conditions.

Keywords: *Seismic wave attenuation; microtremor; local site effects; b-value*

*Ufuk Aydin** *(uaydin@atauni.edu.tr), https://orcid.org/0000-0001-7981-9550;*
Caglar Ozer https://orcid.org/0000-0001-5401-2013;
Department of Civil Engineering, Engineering Faculty, Atatürk University, Erzurum 25240, Türkiye
Erdem Bayrak https://orcid.org/0000-0001-9907-1463,
Department of Civil Engineering, Engineering Faculty; Earthquake Research Centre, Atatürk University, Erzurum 25240, Türkiye

**Corresponding author*

INTRODUCTION

There are many factors that affect the reduction in seismic waves amplitudes in the environments they pass through, and changes in these factors significantly alter absorption values (Toksoz, Johnston 1981). The rate of reduction in seismic wave amplitude contains important information about absorption situation (Aki 1969). Absorption studies provide valuable information about the lithosphere on a large scale (Aydin 2015; Aydin *et al*. 2020; Aydin 2022), and when considered together with the ground acceleration generated during an earthquake, they can provide information about the earthquake force transmitted to engineering structures (Ozer *et al*. 2022a).

Seismic hazard studies can be categorized into two main areas: firstly, the length, depth, epicentre and hypocentre areas of seismic fault zones, the return periods of destructive and large earthquakes, and the type of earthquake focal mechanism; and secondly,

the reduction in seismic amplitude and damping ratio of earthquake waves under the control of the medium through which elastic deformation energy passes. In this study, the seismic absorption coefficients of these systems in the seismic regime of Erzurum and its surroundings were determined. The dynamic behaviour of the soil varies depending on geological formation characteristics, event magnitude, and regional absorption coefficient, as well as soil dynamic features. Although earthquake energy attenuates with increasing absorption, the resulting ground motion may be amplified or reduced depending on the static and dynamic properties of the soil. Regional absorption also depends on parameters such as soil stress/strain loads on which structures are placed, density, stiffness, temperature, and void ratio.

In this study, the regional absorption coefficient of the earthquake wave, seismic hazard parameters, soil dominant frequency and soil amplification factor values were evaluated together. To determine the dynamic behaviour of the soil, the Nakamura (1989) method, based on microtremor records analyzed using the Horizontal/Vertical (H/V) spectral ratio technique (Nakamura 1989), was used. The a- and b-values, known as the Gutenberg-Richter (1944) law, were calculated using the spatial distribution of earthquake magnitudes. Information regarding the stress state of the study area was presented using the b-value (Ogata *et al*. 1991). The probability of the largest earthquake occurring was determined from the frequency-magnitude method, and the regional H/V spectral ratio and regional seismic absorption coefficients were evaluated in an integrated manner.

In particular, approaches that combine regional attenuation characteristic and seismic hazard analysis with Nakamura method-based soil dynamic parameters have not been investigated for Erzurum and its surroundings. This study aims to contribute to a more comprehensive assessment of seismic hazard by considering soil dynamic properties obtained from attenuation coefficient, b-value, and microtremor data together. While attenuation studies and Nakamura method-based site characterization have each been applied extensively in seismically active regions, they are rarely brought together within a unified hazard assessment framework.

TECTONIC SETTINGS

The seismic zones formed by tectonic movements in Anatolia are expressed in six main regimes: the Aegean Graben System (AGS), the Bitlis-Zagros Suture Zone (BZSZ), the East Anatolian Fault Zone (EAFZ), the Hellenic Cyprus Arc (HCA), and the North Anatolian Fault Zone (NAFZ) (Sengor 1979; Taymaz *et al*. 1991; Sengor, Natal 1996; Kocyigit *et al*. 2001; Duman, Emre 2013; Bohnhoff *et al*. 2016; Emre *et al*. 2018). In the study area, the Arabian-Eurasian collision, which began in the Upper Cretaceous period, caused the Anatolian plate to move west-southwest through the North Anatolian Fault Zone (NAFZ) and the East Anatolian Fault Zone (EAFZ) (Sengor 1979; Reilinger *et al*. 1997; Allen *et al*. 2004; Duman, Emre 2013; Bohnhoff *et al*. 2016; Emre *et al*. 2018). The BZSZ, the EAFZ, and NAFZ which cuts across Anatolia, are the most important tectonic units formed in the central, eastern, and south-eastern parts of the Anatolian plate (Arpat, Saroglu 1972; McKenzie 1972; Sengor *et al*. 2005; Duman, Emre 2013; Emre *et al*. 2018). Türkiye is located in the Alpine-Himalayan system, an active seismic region, and is squeezed between the Arabian plate, which pushes the Anatolian plate, and the Eurasian continent (Whitney *et al*. 2023). The study area contains active tectonism that is rising and fracturing under the shear effects of two major fault zones (NAFZ and EAFZ), in addition to the Caucasus Block, which is uplifted by the compressional effect of the BZBZ. In addition, the important tectonic units passing through or very close to the city centre of Erzurum can be listed from west to east as follows: Tercan Fault, Askale Fault, Cat Fault, Palandoken Fault, Dumlu Segment, Nenehatun Segment, Pasinler Fault, Karayazi Fault, and Horasan Fault (Kocyigit, Canoglu 2017) (Fig. 1). Erzurum province is known to have thick alluvium (Yarbasi, Kalkan 2009; Akbas *et al*. 2011; Aydin *et al*. 2025), and is a settlement area that could exhibit a site effect in the event of a potentially destructive earthquake.

METHODS

Three different seismological methods were used in the study. First, the effect of distance-dependent absorption of earthquake energy was evaluated; second, some earthquake hazard parameters were considered; and finally, information on soil dominant frequency and soil amplification factor, related to the dynamic properties of the soil, was evaluated together. The three different methods described below were used to examine the seismological characteristics of Erzurum province and its surrounding areas.

Seismic absorption method

In this study, the seismic absorption coefficient will be calculated using the time-dependent reduction method of seismic wave amplitudes. In this study, the seismic attenuation coefficient was calculated based on Sg wave amplitudes. After selecting suitable earthquake records, the Sg phase was determined, maximum amplitudes were measured, and the

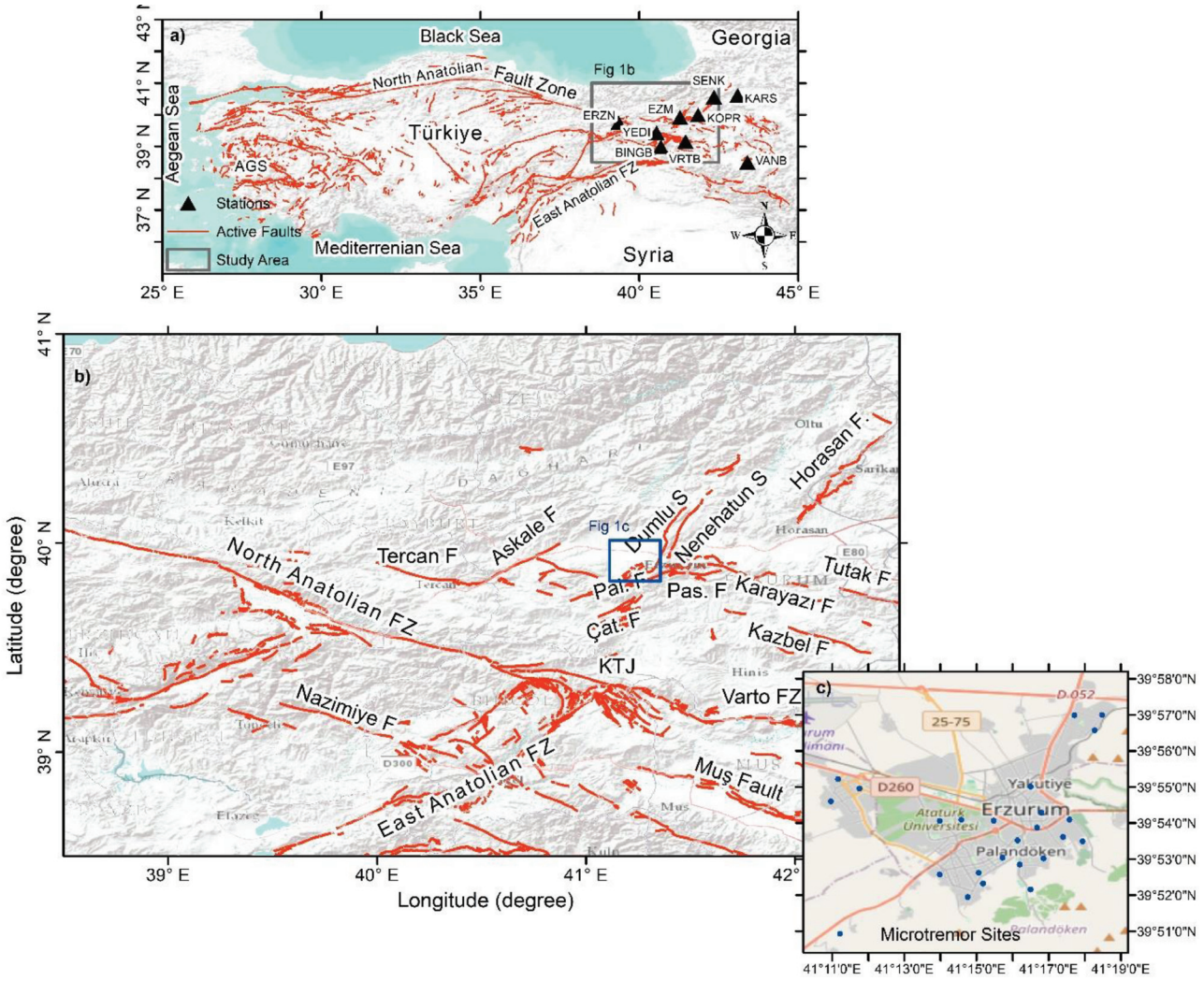

Fig. 1 Türkiye (a), study area tectonic units (b) (after Emre *et al*. 2013, 2018), and microtremor measurements (c). Red lines indicate active tectonic units, while triangular symbols represent the seismic stations used in absorption analyses presented in Table 1. The blue rectangle indicates the area where microtremor studies were conducted. Abbreviations: F – fault, FZ – fault zone, KTJ – Karliova Triple Junction, Pal. – Palandoken, Pas. – Pasinler, S – segment

attenuation coefficient was obtained using the amplitude reduction depending on the epicentre distances; Sg waves were preferred because they exhibit stable propagation over regional distances and provide reliable amplitude measurements. This approach follows the method previously applied in Eastern Anatolia by Aydin (2016), here extended with a focus on the Erzurum basin.

Seismic absorption (Aki, Richards 1980):

$$A(x, t) = A_0 e^{i(kx-wt)} \quad (1)$$

where A_0 is the focal amplitude at $t = 0$ at a distance $x = 0$, w is the angular frequency, and k is the wave number.

The seismic absorption, which can be expressed in terms of k and frequency, can be written as follows (Toksoz, Johnston 1981):

$$k = k_r + i\delta \quad (2)$$

where δ is the seismic absorption coefficient, and k (ω/v) are used to calculate the path-dependent terms in the relevant equation (Aki, Richards 1980):

$$A(x) = A_0 e^{-\delta x} \quad (3)$$

where the amplitudes at distances $x1$ and $x2$ ($x_1 > x_2$) are $A(x_1)$ and $A(x_2)$:

$$\delta(km^{-1}) = \frac{1}{x_2 - x_1} \ln\left[\frac{A(x_1)}{A(x_2)}\right] \quad (4)$$

Gutenberg-Richter relationship

The Gutenberg-Richter method (Gutenberg, Richter 1944), which describes the magnitude-frequency distribution of earthquakes, is expressed in Equation (5). This relationship is considered to reflect fundamental aspects of earthquake physics (Mogi 1962).

$$\mathrm{Log}N = a - b*M \quad (5)$$

where M represents the magnitude, N represents the cumulative number of earthquakes, and a- and b- are constant regression coefficients.

Various approaches have been developed for estimating the b-value (Gutenberg, Richter 1944), with the Least Squares and Maximum Likelihood methods being the most widely applied. The Maximum Likelihood method, which is more widely accepted and frequently used worldwide (Ozturk *et al*. 2008; Ozturk 2013; Ormeni *et al*. 2017; Alkan, Bayrak 2022), calculates the b-value using the following formula (Aki 1965):

$$b = \frac{1}{\log_{10}\left[\overline{M} - \left(M_{\min} - \Delta m / 2\right)\right]} \tag{6}$$

Here $M_{\min}$ represents the cut-off magnitude, $\overline{M}$ is the average magnitude, and Δm is the magnitude range. In this study, the completeness magnitude (Mc) was determined using the maximum curvature method. Mc values were derived from frequency-magnitude distributions for each region. The earthquake catalogue data was declustered using the Reasenberg (1985) algorithm to eliminate the effects of aftershocks and foreshocks. In this process, the time and distance windows commonly used in the literature were taken as the basis, and the default parameters in ZMAP were used (Wiemer 2001).

Seismic hazard parameters

There are different parameters used to determine seismic hazard. These relationships are derived from the Gutenberg-Richter frequency-magnitude law (Gutenberg, Richter 1944) and the Poissonian earthquake occurrence model commonly used in seismic hazard analysis (Cornell 1968; Kramer 1996). If seismic hazard is continuous for years in a region, then the annual value of 'a' for that region is:

$$a_1 - a = \log t \tag{7}$$

It can be calculated from the relationship. The probability of an earthquake of magnitude greater than M occurring in time t is:

$$P_t = 1 - \exp(-10^{a_1 - bM} t) \tag{8}$$

It can be defined as follows: The magnitude of the largest possible earthquake at time t, calculated from the parameters a- and b- derived from the Gutenberg-Richter relationship, is:

$$M_t = \frac{a_1 + \log t}{b} \tag{9}$$

It is given by the equation. The return period of an earthquake with magnitude M is:

$$T_m = \frac{10^{bM}}{10^{a_1}} \tag{10}$$

Microtremor analyses (Nakamura method)

The concept of microtremor is used for vibrations with periods ranging from 0.05 to 2 seconds and amplitudes ranging from 0.01 to 1 micron (Nakamura 1989, 2019). One of the most important advantages of microtremor measurements is that it can vary according to the geological and dynamic properties of the soil at the point level. High effectiveness has been demonstrated in the investigation of soil properties in sedimentary units (Nakamura 1989; Lermo, Chavez-Garcia 1994a, b; Nakamura 2019; Bekler *et al*. 2019; Buyuksarac *et al*. 2021; Bayrak, Coban 2023; Sarac, Ozer 2024; Karsli, Bayrak 2024; Bektas *et al*. 2025; Pamuk *et al*. 2026; Coban *et al*. 2026). Nakamura (1989) emphasized that the soil features can be obtained by dividing the square root of the sum of the squares of the horizontal components by the vertical component seismic noise record. The basic approach here is based on the fundamental assumption that horizontal component records are more affected by ground effects than vertical components and that the seismic velocity of the layered model underground increases with depth. The Horizontal/Vertical Spectral Ratio (HVSR) can be calculated as shown in Equation (11) (Nakamura 1989):

$$HVSR = \frac{\sqrt{(NS^2 + EW^2)}}{V} \tag{11}$$

where NS represents the north-south component, EW denotes the east-west component, and V indicates the vertical component. Microtremor measurements were taken for a minimum of 30 minutes using the Guralp CMG-6TD equipment with a 100 Hz sampling interval. In areas with high cultural noise, this period was extended based on field conditions. In the *HVSR* analyses, spectral smoothing was performed using the Konno-Ohmachi method (Konno, Ohmachi 1998). Time windows were evaluated in accordance with the SESAME (2004) criteria (Acerra *et al*. 2004); windows with low signal-to-noise ratios, containing temporary noise or exhibiting unstable spectral behaviour were excluded from the analysis. 25- and 50-second windows were used during the evaluation phase. The HVSR analyses were performed using the GEOPSY software (Wathelet *et al*. 2020).

RESULTS

Seismic absorption results

The digital earthquake data used in seismic absorption analyses were obtained from the website of the Kandilli Observatory and Earthquake Research Institute (KRDAE). The maximum vertical amplitudes of the Sg waves of the earthquakes used in the

study were determined. The epicentre distances of the earthquakes were recalculated using a spherical coordinate system to suit the purpose of the study. Epicentral distances of 20–180 km and focal depths of 1–25 km were adopted as the primary selection criteria for Sg wave analysis; however, a limited number of records slightly outside these ranges were also included to preserve data continuity, without introducing any meaningful bias to the results.

The epicentre distances of the 535 earthquakes used in the study ranged from 9–202 km, focal depths from 1–25 km, and magnitudes from 3.3 to 6.7 (Table 1). A total of 1,536 data points recorded at 19 stations were examined in this study. However, due to factors such as station malfunctions, poor data quality, and insufficient data, data from only 9 stations could be used. Out of 1,536 earthquake records from 19 stations, 535 events from 9 stations satisfied the selection criteria and were included in the analysis. A significant difference was observed in the attenuation rate of seismic wave energy between stations in and around Erzurum. The regions with a high absorption coefficient (YEDİ) lose more energy from earthquake waves, while regions with low values (ERZN and VANB) allow the wave energy to be transmitted over longer distances. This situation should be related to local soil conditions and geological heterogeneity (Table 1; Fig. 2). When station locations are considered alongside the regional geology, this heterogeneity becomes more interpretable. The YEDİ station, which yielded the highest absorption coefficient (0.0421), is situated in a zone closely associated with the Yedisu seismic gap (Alkan *et al*. 2023). A high degree of fracturing and the presence of fluids in such fault-controlled environments are well-known factors that accelerate seismic energy dissipation.

Table 1 Information on seismic stations for seismic absorption coefficient values

No	Seismic stations	Number of events	Latitude (° N)	Longitude (° E)	Absorption coefficient
1	SENK	31	40.5614	42.3505	0.0220
2	KARS	34	40.6152	43.0937	0.0266
3	EZM	89	39.9200	41.2800	0.0195
4	ERZN	71	39.7520	39.3535	0.0159
5	KOPR	26	39.9917	41.8535	0.0260
6	VRTB	81	39.1603	41.4558	0.0289
7	YEDİ	13	39.4377	40.5443	0.0421
8	BNGB	87	38.9913	40.6792	0.0252
9	VANB	103	38.5090	43.4056	0.0166
–	Total events	535	Average absorption coefficient		0.02475

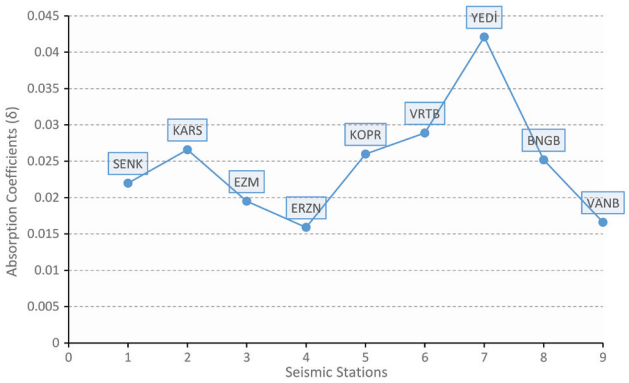

Fig. 2 Attenuation coefficients derived from the seismic stations utilized in this study

Gutenberg-Richter relationship results

The earthquake catalogue used for calculating Gutenberg-Richter parameters using the maximum probability method was the one shared on the website of the KRDAE (URL-1). Since the earthquakes in the catalogue were of different magnitude types, they were first homogenized in terms of moment magnitude (Mw). For this purpose, the magnitude conversion formulas found by Kadirioğlu and Kartal (2016) were used. Kadirioğlu and Kartal (2016) proposed empirical correlations for magnitude conversion using data from approximately 13,000 earthquakes in and around Turkey. They preferred both orthogonal regression and least squares methods for magnitude conversion correlations. The conversion formula from ML to Mw is given below:

$$Mw = 0.8095(\pm 0.025) * ML + 1.3003\ (\pm 0.154) \qquad (12)$$

The resulting catalogue consists of 18,223 earthquakes with magnitudes ranging from 1.7 to 7.7 between 1903 and 2021 (Table 2). Aftershocks and foreshocks were removed from the entire earthquake catalogue before seismic hazard analysis by applying the Reasenberg (1985) declustering algorithm using ZMAP software. The declustered catalogue was used in all analyses, including the calculation of Gutenberg-Richter parameters. As a result of this process, 4,702 foreshocks and aftershocks were removed from the initial event catalogue. Thus, the final event catalogue contains 13,521 earthquakes. The study area was divided into nine different zones, taking into account previous zoning studies (Bayrak *et al*. 2015; Ozturk 2017), the seismicity of the region, and its tectonic characteristics (Coban, Sayil 2020) (Fig. 3). The ZMAP program was used to calculate the statistical seismology parameters (Wiemer 2001).

Figure 4 presents the cumulative number of earthquakes as a function of time for the defined source regions. It is clearly seen that the number of earthquakes in these regions has increased significantly after 2000. This is attributed to the increase in the number of seismic stations used with the development of technology and the fact that even small magnitude

Table 2 Information on seismic field sources that can affect Erzurum and its surroundings

Region number	Tectonic unit	Number of earthquakes	M_{max}^{obs}	Log$N$ = a-bM	Mc	M_{max}^{cal}
1	Askale Fault	1423	5.7	Log$N$ = 7.95–1.44 (± 0.06)*M	3.6	5.5
2	Erzurum-Dumlu-Horasan Fault	1825	6.7	Log$N$ = 6.03–0.905 (± 0.03)*M	3.5	6.7
3	North Anatolian Fault Zone	2953	7.7	Log$N$ = 5.62–0.744 (± 0.01)*M	3.1	7.6
4	Karliova Triple Junction	1348	6.6	Log$N$ = 6.12–0.959 (± 0.03)*M	3.4	6.4
5	Varto-Mus Fault	1646	6.1	Log$N$ = 6.66–1.09 (± 0.04)*M	3.5	6.1
6	Ovacik Fault	1421	6.6	Log$N$ = 6.34–1.05 (± 0.03)*M	3.3	6.1
7	East Anatolian Fault Zone	1797	6.4	Log$N$ = 6.81–1.14 (± 0.03)*M	3.4	6.0
8	Kavakbasi Fault	468	6.6	Log$N$ = 5.19–0.834 (± 0.05)*M	3.3	6.2
9	Trabzon-Bayburt Section	552	5.1	Log$N$ = 7.69–1.54 (± 0.07)*M	3.4	5.0

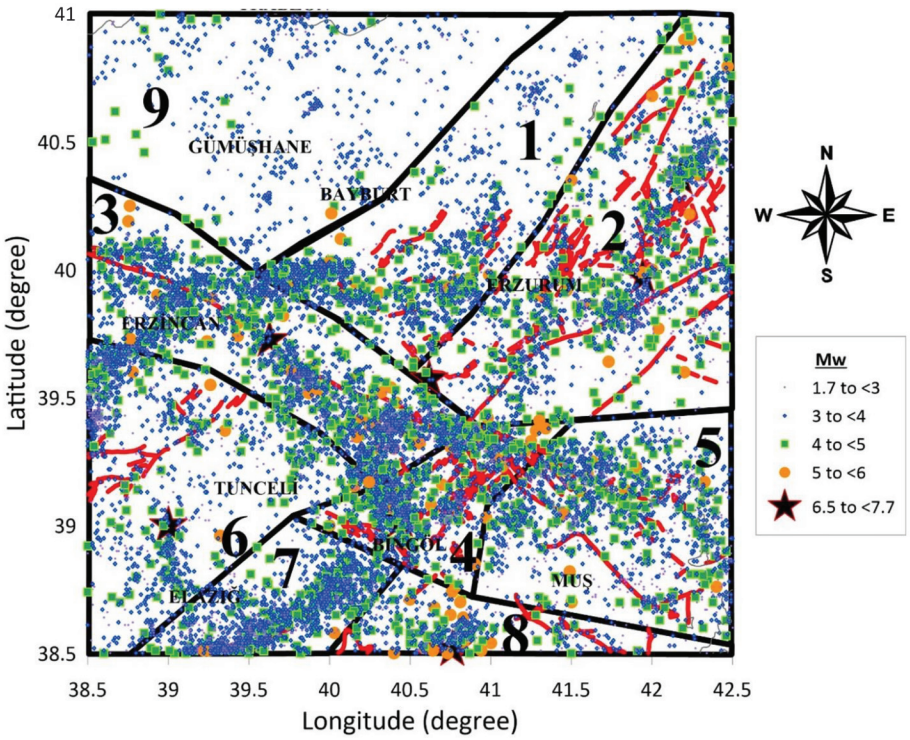

Fig. 3 Potential seismic source zones that may affect Erzurum and its surroundings. Red lines indicate active faults, digitized from Emre *et al*. (2013, 2018). The numbers correspond to region identifiers, with details provided in Table 2

earthquakes have begun to be recorded reliably. The histograms of magnitude-number of earthquakes for different regions are also given in Fig. 5. The magnitude distribution shows that earthquakes generally range between 2.0 and 4.0. The largest earthquake that occurred in the study area was the 1939 Erzincan earthquake with a magnitude of Mw = 7.7 in Region 3 (URL-1).

The a- and b-parameters for the Gutenberg-Richter (G-R) relationship were calculated using the maximum probability method (Fig. 6 and Table 2). The uncertainty of the b values was calculated by following the maximum likelihood approach proposed by Aki (1965), and the explanations ± values represent the standard deviation of the estimates. The smallest b-value was obtained in Region 3, encompassing the NAFZ, with a value of 0.744, while the highest b-value was obtained in Region 9, including the Trabzon-Bayburt section, with a value of 1.54. The shear magnitude (Mc) used in calculating the G-R relationship ranged from 3.1 to 3.6. Based on the b-value, it can be said that the highest stress level is observed in Region 3, while the lowest stress level is observed in Region 9.

The magnitude (M_{max}^{cal}) of the largest earthquake that could occur in the next 120 years was calculated using the calculated a- and b-values (Table 4). The highest value was obtained in Region 3 with 7.6, while the lowest value was obtained in Region 9 with 5.0.

The return periods were calculated for different magnitude values for each region (Table 3 and Fig. 7) using the calculated a- and b-values. The return period for an earthquake equal to or greater than 5.0 was obtained in Region 3 with the shortest value of 2 years, while the longest value of 123 years was obtained in

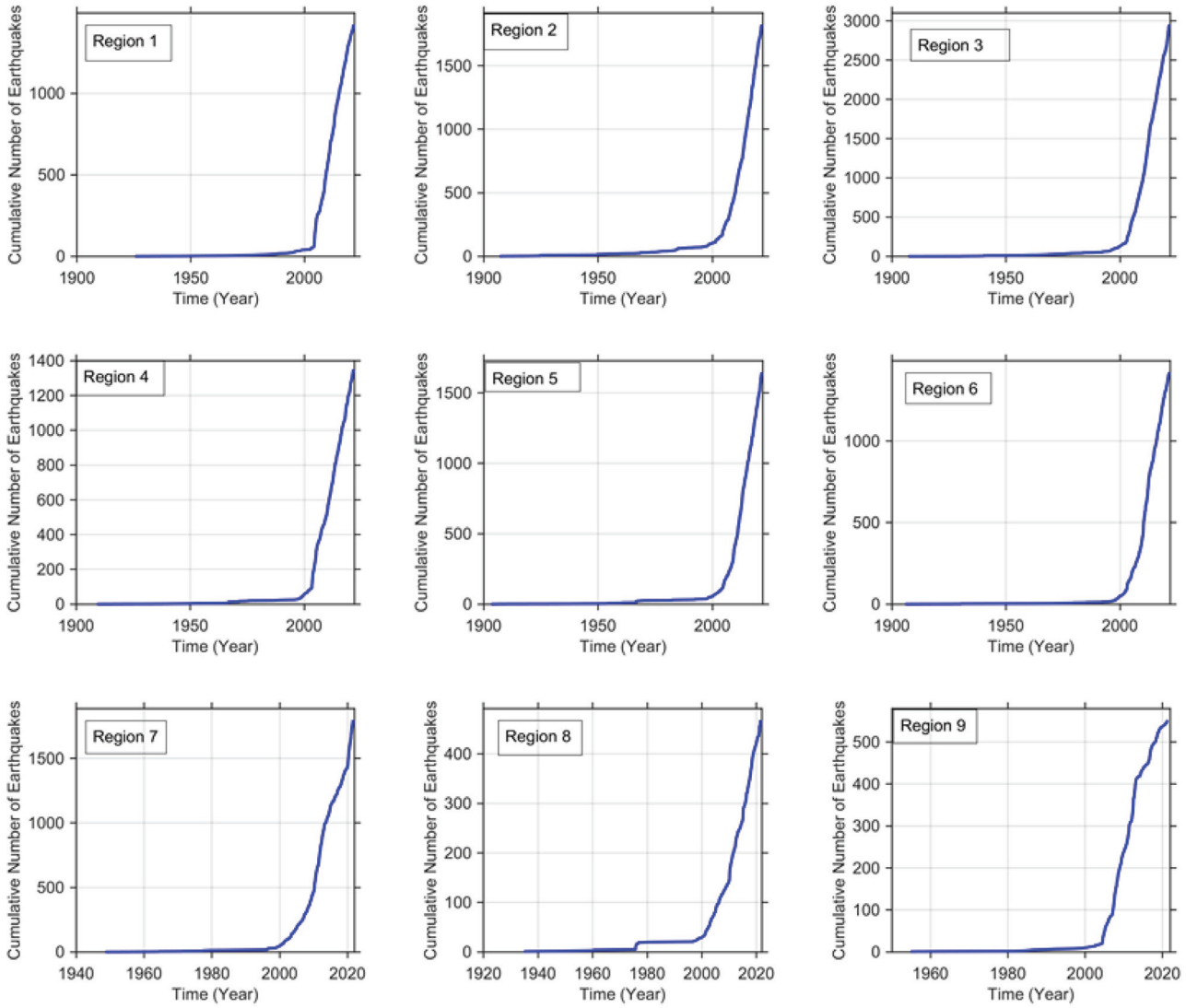

Fig. 4 Time-dependent cumulative earthquake occurrence for the delineated seismic regions

Region 9. The return period for an earthquake equal to or greater than 7.0 was obtained as 46 years in Region 3, while it was calculated to be approximately 1800 years in Region 7.

The probability of an earthquake of magnitude M or greater occurring at time t was calculated for different regions created for the study area (Table 4 and Fig. 8). Table 4 shows the probabilities of earthquakes of magnitudes 5.0, 6.0, 6.5, 7.0, and 7.5 occurring in 25-, 50-, and 100-year periods. The probability of an earthquake of magnitude 5.0 or greater occurring in 25 years was calculated as the smallest in Region 9 with 0.18, while it was calculated as 1.0 in Regions 2 and 3. The probability of an earthquake of magnitude 7.0 or greater occurring in 100 years was obtained as the smallest in Region 7 with 0.05, while the highest value was obtained in Region 3 with 0.88.

Table 3 Region-specific return periods associated with earthquakes exceeding selected magnitude thresholds (blank entries in the table indicate that no earthquakes of that magnitude occurred in the area, and therefore no calculations were performed)

Region	M ≥ 5.0	M ≥ 6.0	M ≥ 6.5	M ≥ 7.0	M ≥ 7.5
1	21	590	–	–	–
2	4	30	85	242	–
3	2	8	20	46	110
4	6	52	156	470	–
5	7	91	320	–	–
6	10	110	367	1220	–
7	9	129	477	1770	–
8	11	78	205	533	–
9	123	4260	–	–	–

Microtremor results

Eight sub-regions were delineated for the measurement plan, taking into account settlement distribution and population density within the Erzurum city limits. Three microtremor measurements were taken in each of the determined areas. In selecting

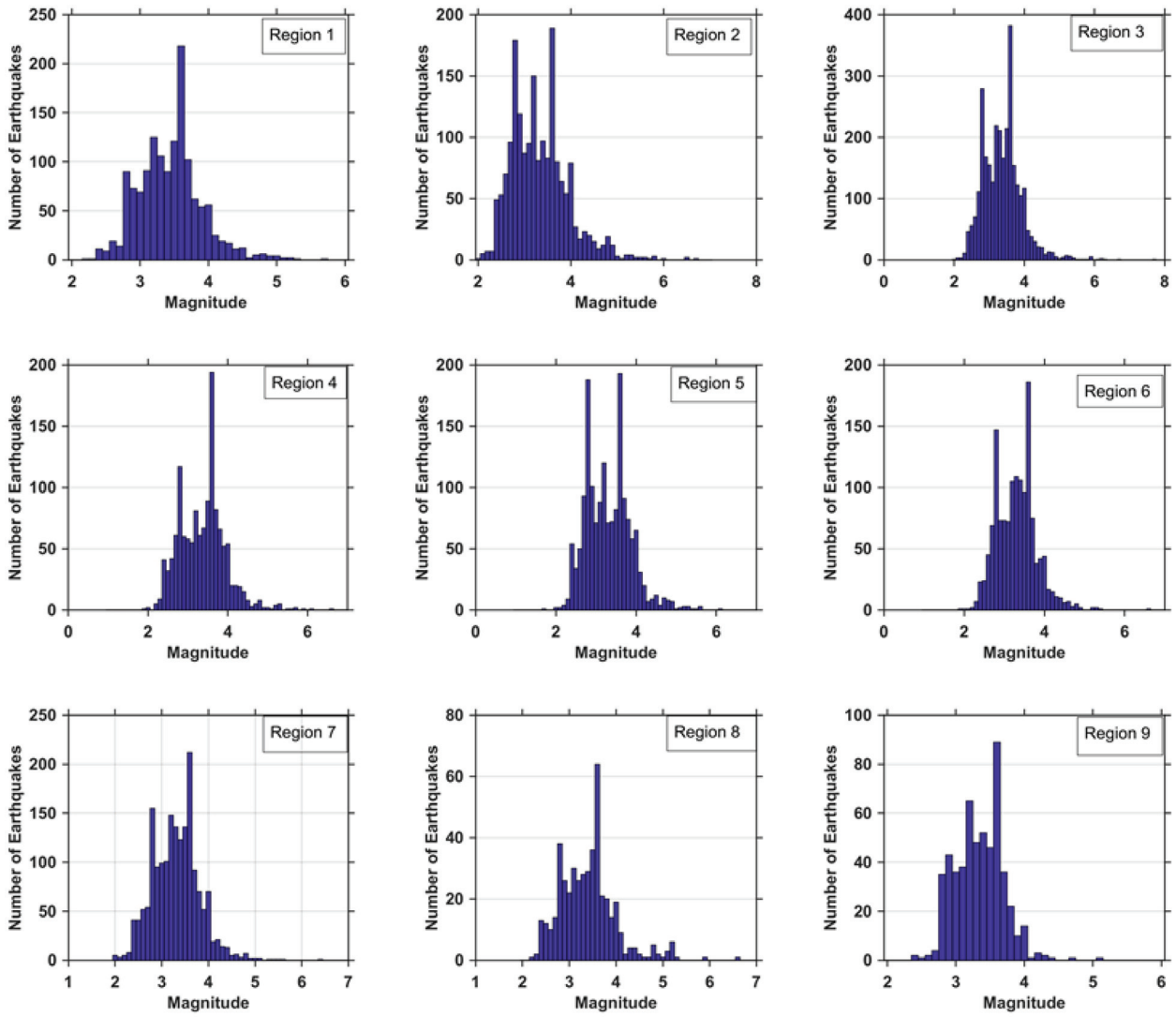

Fig. 5 Magnitude-frequency relationships for the delineated seismic regions

Table 4 Probabilities of occurrence for earthquakes exceeding different magnitude values in each region, calculated for 25-, 50-, and 100-year return periods (the bold numbers represent the highest probabilities of occurrence for earthquakes exceeding M ≥ 6.5, blank entries in the table indicate that no earthquakes of that magnitude occurred in the respective region, and therefore no calculations were performed)

	M = 5.0			M = 6.0			M = 6.5			M = 7.0			M = 7.5		
Year	25	50	100	25	50	100	25	50	100	25	50	100	25	50	100
Region	P_{25}	P_{50}	P_{100}	P_{25}	P_{50}	P_{100}	P_{25}	P_{50}	P_{100}	P_{25}	P_{50}	P_{100}	P_{25}	P_{50}	P_{100}
1	0.69	0.90	0.99	0.04	0.08	0.16	–	–	–	–	–	–	–	–	–
2	1.00	1.00	1.00	0.56	0.81	0.96	0.25	0.44	0.69	0.10	0.19	0.34	–	–	–
3	1.00	1.00	1.00	0.95	1.00	1.00	0.72	0.92	0.99	0.42	0.66	0.88	0.20	0.37	0.60
4	0.99	1.00	1.00	0.38	0.62	0.91	0.15	0.27	0.47	0.05	0.10	0.19	–	–	–
5	0.97	1.00	1.00	0.24	0.42	0.67	0.08	0.14	0.27	–	–	–	–	–	–
6	0.92	0.99	1.00	0.20	0.37	0.60	0.07	0.13	0.24	0.02	0.04	0.08	–	–	–
7	0.93	1.00	1.00	0.18	0.32	0.54	0.05	0.10	0.19	0.01	0.03	0.05	–	–	–
8	0.89	0.99	1.00	0.27	0.47	0.72	0.12	0.22	0.39	0.05	0.09	0.17	–	–	–
9	0.18	0.33	0.56	0.01	0.01	0.02	–	–	–	–	–	–	–	–	–

the three points within the region, priority was given to selecting formations that may have geological differences. Although the results obtained from the study do not constitute microzonation in nature when investigating different regions in Erzurum, the study outputs provide an important basis for future studies on the dynamic properties of the soil in Erzurum (Fig. 9).

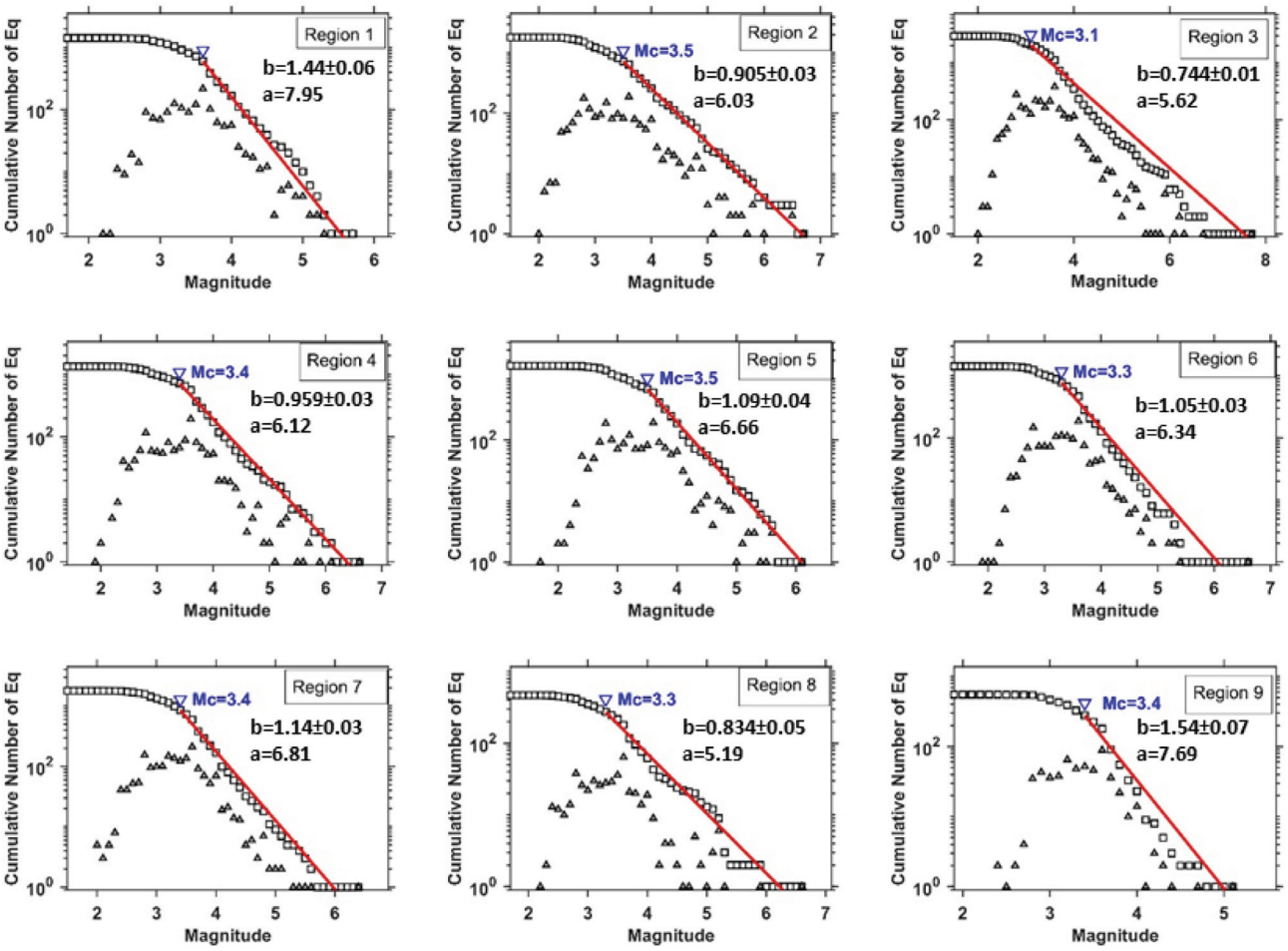

Fig. 6 The *b*-value graphs obtained for each region

Within the Hilalkent microtremor dataset (points 1, 2, and 3), measurements 1 and 2, acquired on undifferentiated volcanic units, exhibit a near-flat spectral response. In measurement number 3, applied on undifferentiated terrestrial clastics, a soil amplification factor of approximately 7.5 was calculated at approximately 2.4 Hz. This is the highest soil amplification factor calculated at this point among the 24 measurement points in Erzurum and its surroundings. While the higher parts of Hilalkent are generally located on volcanics and andesites, the industrial area is generally located on terrestrial clastics and alluvium (Akbas *et al*. 2011). The discrepancy in the anomaly character between measurements number 1 and 2 and measurement number 3 is thought to be due to site effects and the presence of different tectonic and geological units (Figs 10 and 11).

The Abdurrahman Gazi region (measurement points 4, 5, and 6) is generally characterized by high altitudes surrounded by terrestrial clastics and andesites, while the lowland area is covered with alluvium (Akbas *et al*. 2011). In microtremor measurements conducted in the Abdurrahman Gazi region, a soil amplification factor of approximately 2.4 was calculated at approximately 5.3 Hz in measurement number 4. Measurements 5 and 6 show a similar flat character (Figs 10 and 11).

The Dadaskent region, located at points 7, 8, and 9, is a settlement area with a very low groundwater level (near the surface) and mostly built on alluvial units (Akbas *et al*. 2011; Aydin *et al*. 2025). A comparison of the obtained microtremor results with other measurements across Erzurum indicates that the Dadaskent region is particularly critical in terms of earthquake-soil-structure interaction. Significant soil amplification factors below 1 Hz were calculated in all three measurements. The soil amplification factor observed at low frequencies (< 1 hz) represent loose soils. This situation suggests that the calculation and design of forces under dynamic loads in the Dadaskent region is a phenomenon that requires special attention (Figs 10 and 11).

The Kayakyolu region (measurement points 10, 11, and 12) is located on Terrestrial Clastics. The transition between Andesites and Volcanites in the higher elevations and Terrestrial Clastics is governed by the Palandoken Fault Zone (PFZ) (Akbas *et al*. 2011; Emre *et al*. 2013). Measurements 10 and 11 show similar characteristics and exhibit a slight soil amplification at ~ 0.3 and ~ 1.1 Hz (~ 2). Measure-

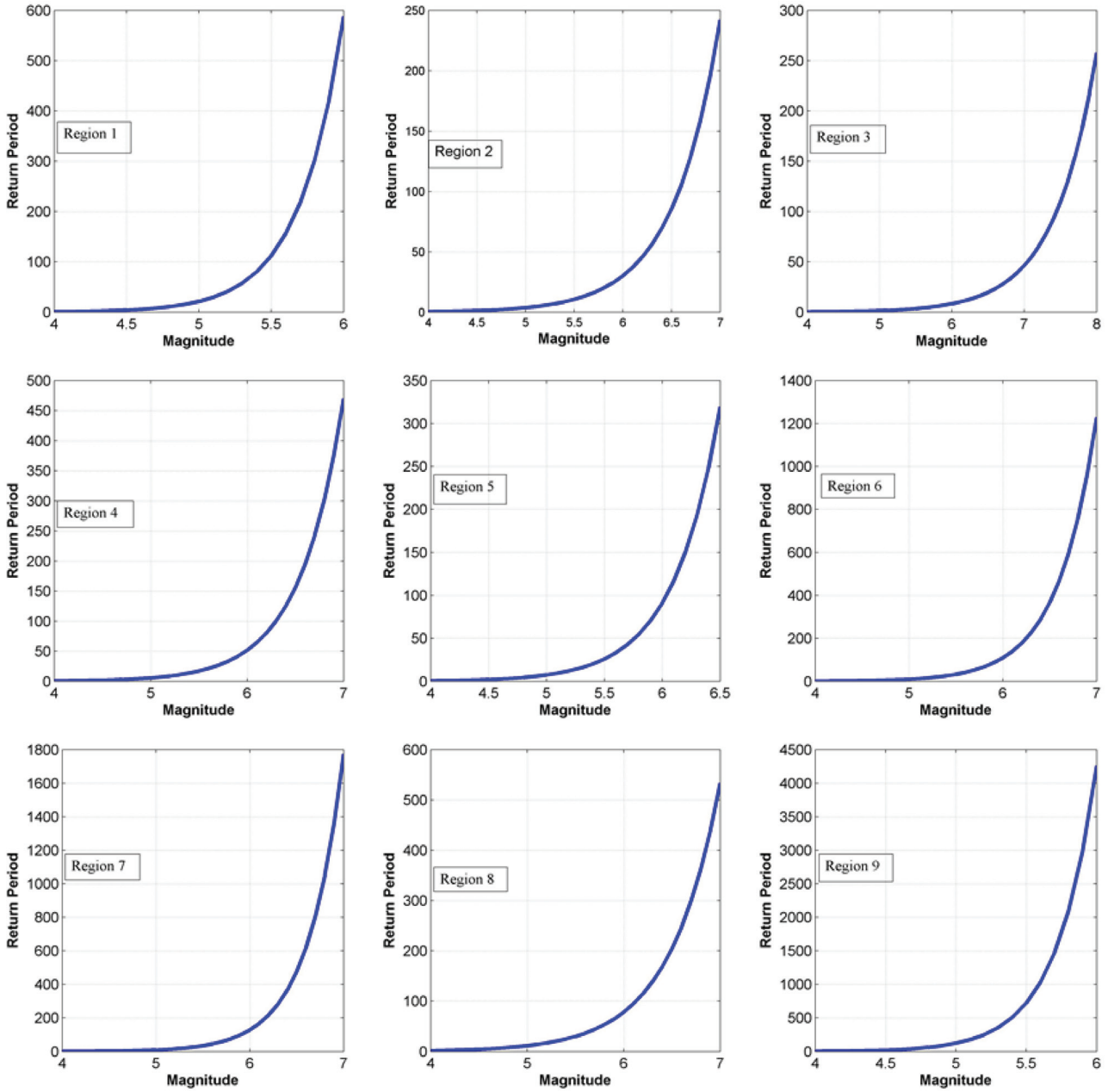

Fig. 7 Region-specific magnitude-return period curves derived from seismic hazard analysis

ment 12 was applied on the peak bounded by the PFZ. Formation transitions can be observed here from the field geology. At this location, a soil amplification factor of ~ 3.6 was identified at a frequency of approximately 1.1 Hz (Figs 10 and 11).

The Yildizkent area (measurement points 13, 14, and 15) is mostly located on terrestrial clastic deposits and is situated close to the PFZ (Akbas *et al*. 2011; Emre *et al*. 2013). All measurements carried out here are of a similar character, with soil amplificaiton factors ranging from ~ 1 to ~ 2.5 (Figs 10 and 11).

The university area (measurement points 16, 17, and 18) encompasses the central campus of Ataturk University. Studies conducted in this area indicate that the soil amplificaiton factor can be observed at low frequencies (Figs 10 and 11).

The Yenisehir region (measurement points 19, 20, and 21) is mostly located on terrestrial clastic deposits (Akbas *et al*. 2011). The three microtremor measurements conducted at this site suggest that the soil may exhibit approximately twofold amplification under dynamic loading conditions (Figs 10 and 11).

The area in the city centre (measurement points 22, 23, and 24) is mostly located on alluvium and terrestrial clastic deposits (Akbas *et al*. 2011). Measurements taken at only three points show that the soil can exhibit a high soil amplification factor at low frequencies. At measurement point 22, located in an area with a high concentration of historical structures (Er-

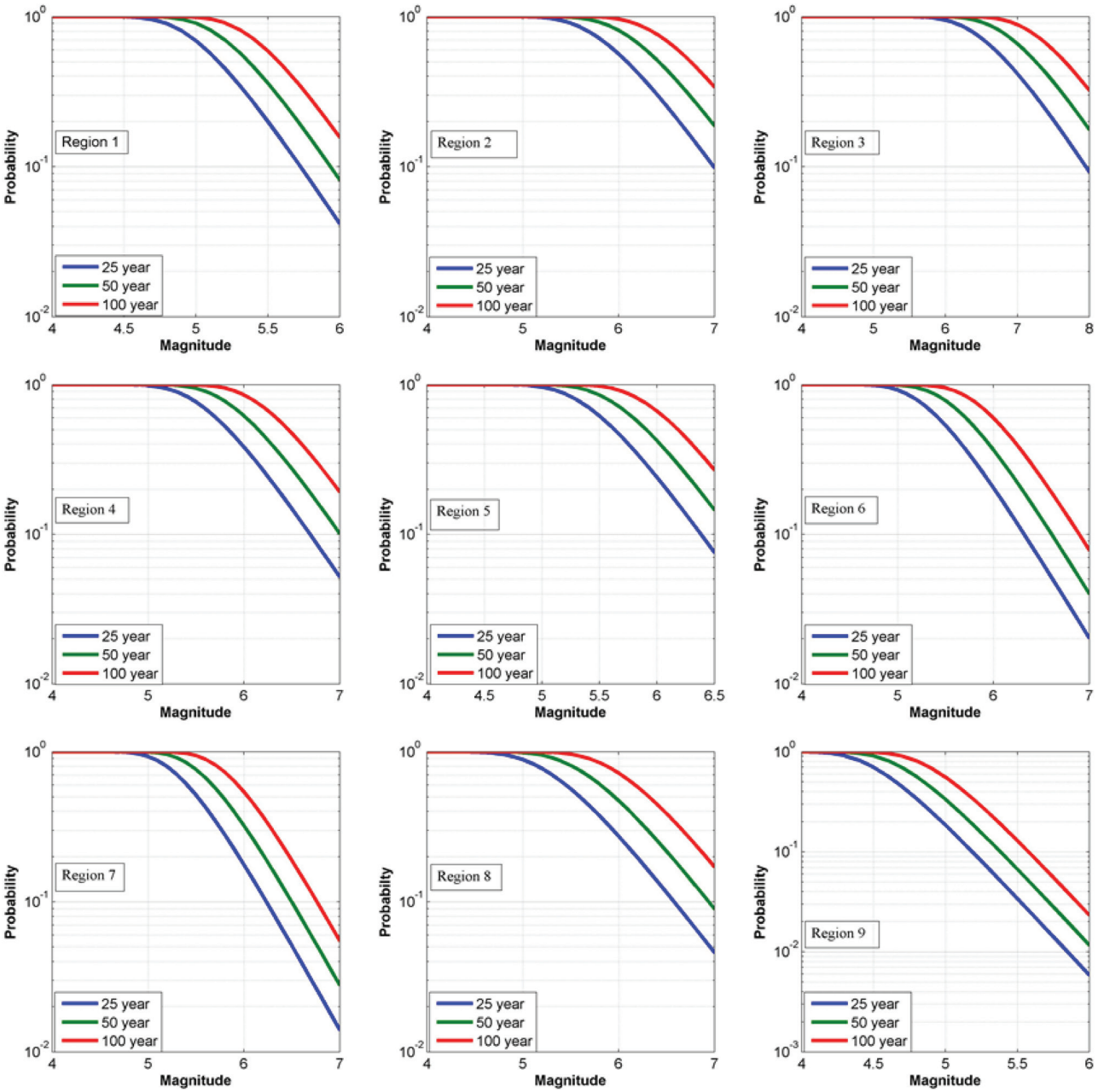

Fig. 8 Probabilities of occurrence of seismic events with magnitudes equal to or exceeding a specified value for return periods of 25, 50, and 100 years

zurum Castle, Twin Minarets, Historical Mosques), two significant anomalies are observed. The first is an anomaly that becomes prominent at approximately 0.4 Hz and has a soil amplification factor of approximately 2.5. The second is an anomaly located between 3 and 4 Hz and has a soil amplification factor of approximately 3. In areas with a high concentration of historical structures, the dynamic properties of the soil should be assessed prior to any soil improvement interventions (Figs 10 and 11). Given the potential deficiencies in the building stock due to the city centre and Yenisehir districts being old settlement areas and because it is not possible to define a very large area in only three points considering population density, it is important for Erzurum to carry out a microzoning study specific to the city centre and Yenisehir districts in the future (Figs 10 and 11).

DISCUSSION

In this study, the seismic hazard in Erzurum and its vicinity was evaluated and interpreted in an integrated manner, considering seismic attenuation (absorption) coefficients, Gutenberg-Richter (b-value) parameters, and local soil dynamic characteristics (microtremor). The average seismic attenuation coefficient of 0.02475 obtained from 535 earthquake data points proves that seismic wave propagation in

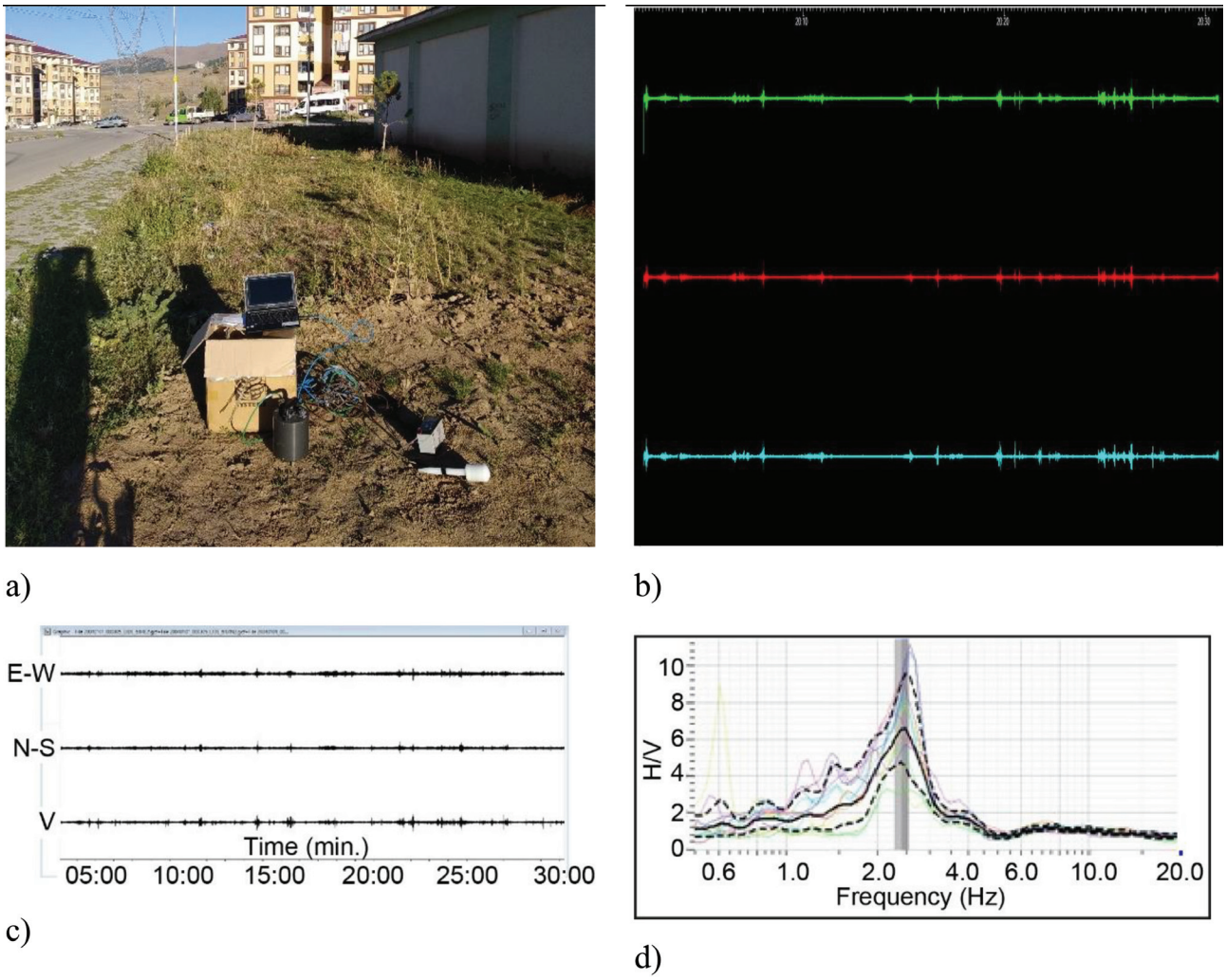

Fig. 9 Example microtremor field measurements conducted in Erzurum city center: field deployment (a), sample raw microtremor data from Erzurum city centre (Scream algorithm view) (b), processing stage using Geopsy software (Wathelet *et al*. 2020) (c), and sample result visualization (d)

Erzurum and its vicinity is not homogeneous and has a varied attenuation character. The fact that seismic wave absorption is low in the east (VANB) and west (ERZN), while it is high in the north and south directions, demonstrates the geological complexity of the study area. The high attenuation values observed in Fig. 2, particularly around the YEDİ station, are consistent with active fault zones and lithological units with high fracture density, indicating the presence of fluid and the influence of weak zones in these areas (Aydin 2015; Aydin *et al*. 2020). In contrast, the low attenuation values obtained around ERZN and VANB suggest the presence of more rigid and compact units. Similarly, local earthquake tomography and magnetic anomaly studies conducted in the region by Ozer *et al*. (2022b) also revealed low P-wave velocities (Vp) and shallow Curie Point Depths (CPD) in areas such as Tekman, Soylemez, and the north of Karliova. These regional variations in seismic damping values parallel lithospheric changes in the region, such as low seismic velocity zones, the presence of geothermal fluid, and potential magma chambers (Karaoglu *et al*. 2018, 2026).

The average absorption coefficient of 0.02475 obtained in this study is somewhat higher than that reported by Aydin (2016), a difference likely reflecting the inclusion of stations in geologically more heterogeneous zones around Erzurum. The active tectonic structure in Eastern Anatolia, Türkiye, yields two key findings from this study. First, the mean attenuation coefficient of 0.02475, and especially its spatial variation, is consistent with the view of a relatively thin and thermally disturbed lithosphere in this region. High heat flow, shallow Curie depths, and geothermal anomalies may point to a crust that has undergone significant thinning and fluid infiltration (Bektas *et al*. 2007; Ozer *et al*. 2022b; Karaoglu *et al*. 2018, 2026). It is well known that these conditions increase seismic wave attenuation (Toksoz, Johnston 1981). Second, the low b-value in Zone 3 may reflect the physical

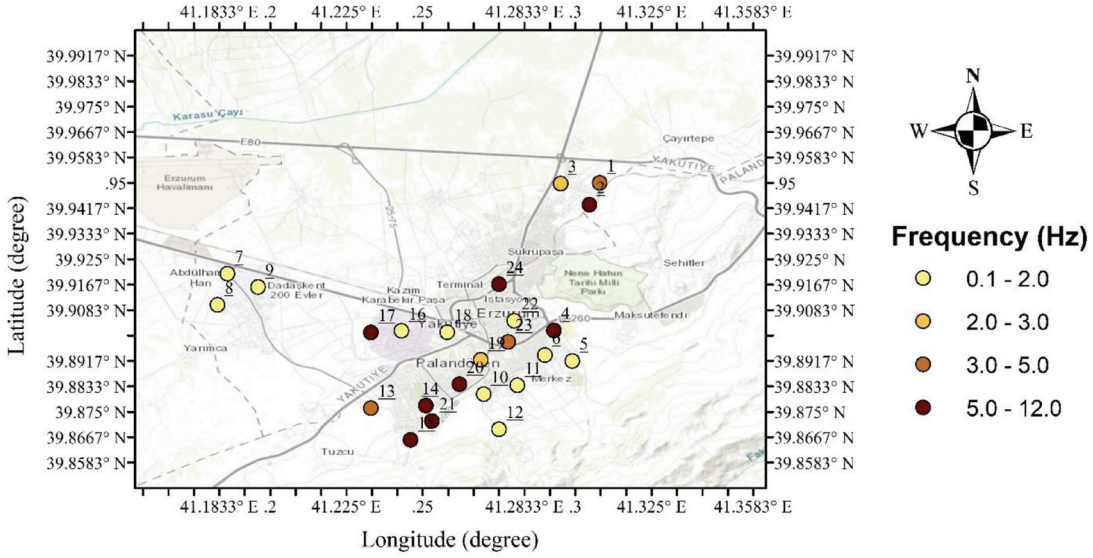

Fig. 10 Soil dominant frequency distribution map for Erzurum city centre. Red lines indicate active faults and were obtained from http://yerbilimleri.mta.gov.tr, based on Emre *et al*. (2013, 2018). The map base was sourced from Esri, USGS, and NOAA

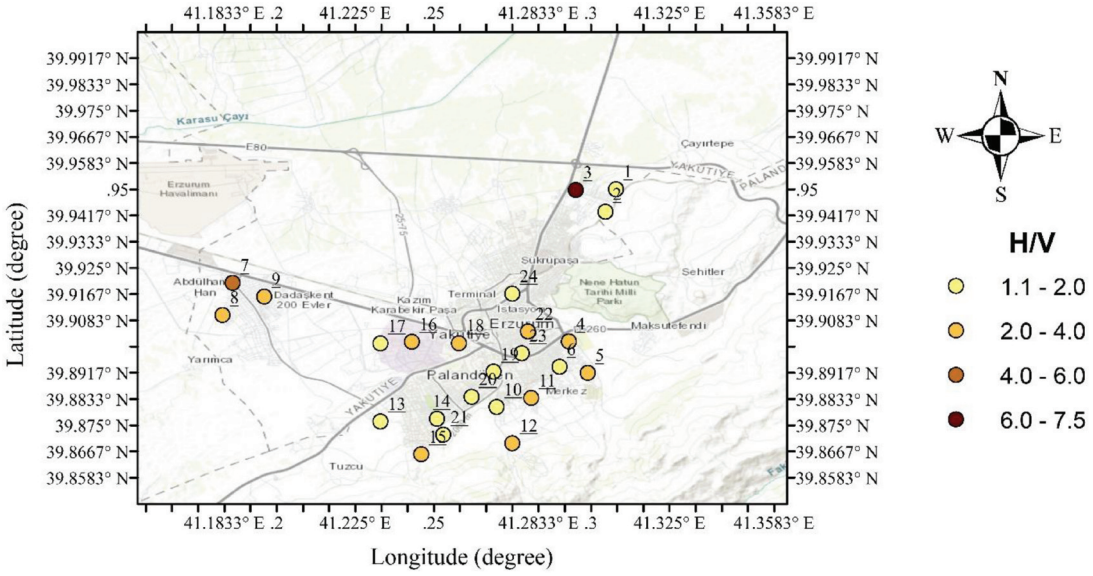

Fig. 11 Soil amplification factor distribution map for Erzurum city centre. Red lines indicate active faults and were obtained from http://yerbilimleri.mta.gov.tr, based on Emre *et al*. (2013, 2018). The map base was sourced from Esri, USGS, and NOAA

outcome of fault system currently under continuous loading. The proximity of Zone 3 to the KTJ, where the NAFZ and EAFZ intersect, reinforces the idea of stress transfer and concentration from multiple directions simultaneously. The Yedisu seismic gap refers to a segment of the NAFZ that has not produced a major rupture and is widely regarded as one of the most seismically important locked segments in Eastern Anatolia (Alkan *et al.* 2023). A long absence of a major rupture along the Yedisu seismic gap, coupled with continuous plate convergence, suggests a significant increase in the stress gap in this segment. A low b-value calculated in this area and a short recurrence interval independently support this finding.

Seismotectonic parameters and *b*-values calculated using the Gutenberg-Richter equation provide important information about stress accumulation in the region. A low b-value (0.74) calculated for Zone 3, which includes the Erzincan section of the NAFZ, and a high earthquake expectation on the NAFZ are in great agreement with other studies in the literature. A large-scale study for the Eastern Mediterranean and the Caucasus also emphasized that low *b*-values ($b \leq 1$) along Eastern Anatolia and the NAFZ indicate active seismic zones and high tectonic stress (Bayrak *et al*. 2020; Ahadov, Ozturk 2022). In addition, this study calculated that an earthquake of magnitude $M \geq 7.0$ for the NAFZ (Zone 3) has an approximate

recurrence period of 46 years. This finding is also particularly important for the Yedisu Seismic Gap, which is located quite close to the Erzurum and Karliova Triple Junction (KTJ). A low b-value obtained in Zone 3 (NAFZ) indicates a high-stress regime associated with active strike-slip tectonics, while the attenuation distribution reflects crustal heterogeneity and possible fluid/thermal effects. The coexistence of a low b-value and relatively low attenuation suggests that seismic energy may be propagated more effectively, potentially increasing the impact of large earthquakes. Alkan *et al*. (2023) observed low b-values (between 0.6 and 1.0) and positive Coulomb stress transfer around the Yedisu segment and reported a recurrence interval of approximately 55 years for an earthquake of magnitude $M = 7.0$, similar to this study. Furthermore, Bayrak *et al*. (2008), using the Gumbel statistical distribution for a hazard analysis across Türkiye, indicated that the central and eastern parts of the NAFZ are in the highest hazard class in terms of future major earthquakes ($M \geq 7.0$). All these regional seismotectonic findings confirm the critical nature of the low *b*-value, seismic damping characteristics, and seismic hazard analysis outputs highlighted in this study (Aydin 2015; Aydin *et al*. 2020).

The dynamic properties of the soil and the seismic hazard results indicate that, considering the local soil dynamics specific to Erzurum, new engineering structures in this area should be supported by detailed soil investigations. Microtremor measurements conducted in 8 different sub-regions within the scope of this study yielded particularly noteworthy results regarding soil-structure interaction, especially in the Dadaskent region. In addition, the low dominant frequency values (<1 Hz) obtained from HVSR measurements in the Dadaşkent region are consistent with low shear wave velocity values corresponding to thick and loose alluvial units. This high soil amplification response at low frequencies is a direct reflection of a thick and loose alluvial soil profile in the region (Aydin *et al.* 2025). Similar low-frequency amplification patterns associated with thick alluvial sequences have been shown in comparable basin settings, where integrated geophysical approaches also revealed considerable sediment thickness over bedrock (Buyuksarac *et al*. 2023). Considering the fact that the Erzurum pull-apart basin consists of thick sedimentary deposits, it is clear that these alluvial units with near-surface groundwater levels would strongly amplify the seismic energy generated by a destructive earthquake originating from the NAFZ or EAFZ. This low frequency range points to a resonance risk with medium and high-rise structures whose natural periods fall within this range. Therefore, it is expected that amplifications caused by soil-structure interaction will become even more pronounced, especially with an increase in high-rise construction. For this reason, urban planning and earthquake design require the evaluation not only of soil properties but also of building height and dynamic behaviour. Furthermore, the observation of different site effect characteristics even at very close points in some areas such as Hilalkent demonstrates the local influence of terrestrial clastics, alluvium, and andesite/volcanite transitions on soil behaviour. This situation shows that not only the distance to fault lines but also site effect studies need to be investigated in detail in densely populated areas of Erzurum province.

CONCLUSIONS

The findings unequivocally demonstrate the severity and multifaceted nature of the seismic risk faced by Erzurum and its surroundings. The low b-values observed in the region, which is under pressure from mega-fault systems such as the North Anatolian Fault Zone (especially the Erzincan and Yedisu faults) and the East Anatolian Fault Zone, indicate a significant accumulation of tectonic stress, raising the macroseismic hazard in the region to critical levels. However, the real destructive threat for Erzurum stems from the local soil dynamics and seismic absorption characteristics at the surface of this macro-scale seismic energy. A complex lithological structure of the Erzurum pull-apart basin and the heterogeneity in the seismic damping coefficient have the potential to exponentially increase the destructive effect of the dynamic forces that a potentially severe earthquake would unleash. In particular, in areas dominated by thick alluvial layers, such as Dadaskent and the city centre, this situation poses a direct risk to the existing building stock. In conclusion, the seismic safety of Erzurum cannot be reduced solely to the magnitude of the fault that will rupture or the distance to fault lines. The findings indicate that in densely populated areas, development strategies urgently need to move beyond classical fault-focused approaches; instead, detailed micro-zoning studies that prioritize local soil dynamics and site impacts are essential. It is also worth noting that the combined use of seismic attenuation and HVSR analyses, though relatively uncommon in regional hazard studies, proved to be a particularly useful aspect of this work.

ACKNOWLEDGMENTS

This study was supported by the Scientific Research Projects Coordination Unit of Ataturk University under the project titled “Seismogenic Structures and Earthquake Hazard Analysis for Erzurum and Its Surroundings” (Project No: FBA-2021-9274). The

author extends sincere thanks to the Ataturk University Earthquake Research Centre for providing seismometer support during the microtremor field investigations. The author also gratefully acknowledges the Kandilli Observatory and Earthquake Research Institute for providing earthquake data (URL-1). Special appreciation is also expressed to Prof. Dr. Albertas Bitinas, Editor-in-Chief of BALTICA Journal, and to the anonymous reviewers for their valuable comments and constructive suggestions, which greatly improved the quality of this manuscript.

Conflict of interests. The authors declare no conflict of interests. In this study, the OpenAI/ChatGPT tool was utilized to assist with language editing and grammar refinement. The author carefully reviewed and revised the output and assumes full responsibility for the final content of the manuscript.

REFERENCES

Acerra, C., Aguacil, G., Anastasiadis, A., Atakan, K., Azzara, R., Bard, P.Y., Zacharopoulos, S. 2004. *Guidelines for the implementation of the H/V spectral ratio technique on ambient vibrations measurements, processing and interpretation.* European Commission-EVG1-CT-2000-00026 SESAME. Brussels, Belgium: European Commission.

Ahadov, B., Ozturk, S. 2022. Spatial variations of fundamental seismotectonic parameters for the earthquake occurrences in the Eastern Mediterranean and Caucasus. *Natural Hazards 111(3),* 2177–2192.

Aki, K. 1965. Maximum likelihood estimate of b in the formula log N = a-bM and its confidence limits. *Bulletin of Earthquake Research Institute Tokyo University 43*, 237–239.

Aki, K. 1969. Analysis of the seismic coda of local earthquakes as scattered waves. *Journal of geophysical research 74(2),* 615–631.

Aki, K., Richards, P.G. 1980. *Quantitative Seismology: Theory and Methods*. Vol. 1, London: W.H. Freeman and Co.

Alkan, H., Bayrak, E. 2022. Coulomb stress changes and magnitude-frequency distribution for Lake Van region. *Bulletin of the Mineral Research and Exploration 168(168),* 141–156.

Alkan, H., Ozturk, S., Akkaya, I. 2023. Seismic hazard implications in and around the Yedisu seismic gap (Eastern Türkiye) based on Coulomb stress changes, b-values, and S-wave velocity. *Pure and Applied Geophysics180(9),* 3227–3248.

Allen, M., Jackson, J., Walker, R. 2004. Late Cenozoic reorganization of the Arabia-Eurasia collision and the comparison of short-term and long-term deformation rates. *Tectonics 23(2),* TC2008.

Arpat, E., Saroglu, F. 1972. Some observations and thoughts on the East Anatolian Fault. *MTA Journal 78*, 33–39 [In Turkish].

Aydin, U. 2015. Estimation of seismodynamics differences and lateral variations of coda Q in Eastern Anatolia. *Arabian Journal of Geosciences 8(8),* 6363–6370.

Aydin, U. 2016. Relationships between geotectonic and seismodynamic characteristics of the crust in the Eastern Anatolia. *Acta Geodaetica et Geophysica 51(1),* 69–79.

Aydin, U. 2022. The seismic anisotropy of the Eastern Anatolia. *Iranian Journal of Science and Technology*, *Transactions of Civil Engineering 46(2),* 1037–1047.

Aydin, U., Sahin, S., Salah, M.K. 2020. Upper crustal Poisson's ratio and coda-wave attenuation beneath Eastern Anatolia. *Earthquake Engineering and Engineering Vibration 19(2),* 335–347.

Aydin, O.L., Karimi, B., Kazaz, I. 2025. Geotechnical and geophysical investigations on local site effects in Erzurum, Türkiye. *Natural Hazards 121(11),* 12837–12861.

Bayrak, E., Coban, K.H. 2023. Evaluation of 08 August 2019 Bozkurt (Denizli-Turkey, Mw 6.0) earthquake in terms of strong ground-motion parameters and Coulomb stress changes. *Environmental Earth Sciences 82(20)*, 470.

Bayrak, Y., Ozturk, S., Cinar, H., Koravos, G.C., Tsapanos, T.M. 2008. Regional variation of the ω-upper bound magnitude of GIII distribution in and around Turkey: tectonic implications for earthquake hazards. *Pure and Applied Geophysics 165(7),* 1367–1390.

Bayrak, E., Yilmaz, S., Softa, M., Turker, T., Bayrak, Y. 2015. Earthquake hazard analysis for East Anatolian fault zone, Turkey. *Natural Hazards 76(2),* 1063–1077.

Bayrak, E., Ozer, C., Perk, S. 2020. Stress tensor and Coulomb analysis for Erzurum and its surroundings. *Turkish Journal of Earthquake Research 2(1),* 101–114.

Bekler, T., Demirci, A., Ekinci, Y.L., Büyüksaraç, A. 2019. Analysis of local site conditions through geophysical parameters at a city under earthquake threat: Çanakkale, NW Turkey. *Journal of Applied Geophysics 163*, 31–39.

Bektas, O., Ravat, D., Buyuksarac, A., Bilim, F., Ates, A. 2007. Regional geothermal characterisation of East Anatolia from aeromagnetic, heat flow and gravity data. *Pure and Applied Geophysics164(5),* 975–998.

Bektas, O., Buyuksarac, A., Saritepe, H. E., Onal, K.M., Canbaz, O., Eyisuren, O., ... Kosaroglu, S. 2025. Shear-wave velocity model of the Sivas City (inner eastern, Türkiye) using Rayleigh wave ellipticity inversion controlled by 2D microgravity modeling. *Acta Geophysica 73(6),* 5593–5611.

Bohnhoff, M., Martínez-Garzón, P., Bulut, F., Stierle, E., Ben-Zion, Y. 2016. Maximum earthquake magnitudes along different sections of the North Anatolian fault zone. *Tectonophysics 674*, 147–165.

Buyuksarac, A., Bekler, T., Demirci, A., Eyisuren, O. 2021. New insights into the dynamic characteristics of alluvial media under the earthquake prone area: a case study for the Çanakkale city settlement (NW of Turkey). *Arabian Journal of Geosciences14(20),* 2086.

Buyuksarac, A., Eyisuren, O., Bektas, O., Karaca, O. 2023. Bedrock depth calculation of Çanakkale (Turkey) basin using Rayleigh ellipticity and microgravity survey. *Geofisica Internaciona l62(1),* 387–401.

Coban, K.H., Sayil, N. 2020. Different probabilistic models for earthquake occurrences along the North and East Anatolian fault zones. *Arabian Journal of Geosciences 13(18)*, 1–16.

Coban, K.H., Bayrak, E., Ramos, H. 2026. Inversion of earthquake H/V spectral ratios for shear wave velocity profiling in Elazig using a dense dataset. *Journal of African Earth Sciences 234*, 105897.

Cornell, C.A. 1968. Engineering seismic risk analysis. *Bulletin of the seismological society of America 58(5),* 1583–1606.

Duman, T.Y., Emre, O . 2013. The East Anatolian fault: Geometry, segmentation and jog characteristics. *Geological Society London Special Publications 372(1),* 495–529.

Emre, O., Duman, T.Y., Ozalp, S., Elmaci, H., Olgun, S., Saroglu, F. 2013. *Annotated Active Fault Map of Turkey. Scale 1:1,250,000*. Ankara-Türkiye: General Directorate of Mineral Research and Exploration, Special Publication Series-30. ISBN: 978-605-5310-56-1 [In Turkish].

Emre, O., Duman, T.Y., Ozalp, S., Saroglu, F., Olgun, S., Elmaci, H., Can, T. 2018. Active fault database of Turkey. *Bulletin of Earthquake Engineering 16(8),* 3229–3275.

Gutenberg, B., Richter, C.F. 1944. Frequency of earthquakes in California. *The Bulletin of the Seismological Society of America 34*, 185–188.

Kadirioglu, F.T., Kartal, R.F. 2016. The new empirical magnitude conversion relations using an improved earthquake catalogue for Turkey and its near vicinity (1900–2012). *Turkish Journal of Earth Science 25(4)*, 300–310.

Karaoglu, O., Browning, J., Salah, M.K., Elshaafi, A., Gudmundsson, A. 2018. Depths of magma chambers at three volcanic provinces in the Karlıova region of Eastern Turkey. *Bulletin of Volcanology 80(9),* 69.

Karaoglu, O., Koulakov, I., Eken, T., Bazargan, M., Gerya, T., Zilio, L.D., Gudmundsson, A. 2026. Fault-controlled magma pathways driving seismicity and eruption risk in Eastern Turkey. *Communications Earth & Environment 7*, 266.

Karsli, F., Bayrak, E. 2024. Single-station microtremor surveys for site characterization: A case study in Erzurum city, eastern Turkey. *Earthquake Engineering and Engineering Vibration23(3),* 563–576.

Kocyigit, A., Canoglu, M.C. 2017. Neotectonics and seismicity of Erzurum pull-apart basin, East Turkey. *Russian Geology and Geophysics 58(1),* 99–122.

Kocyigit, A., Yilmaz, A., Adamia, S. Kuloshvili, S. 2001. Neotectonics of East Anatolian Plateau (Turkey) and Lesser Caucasus: implication for transition from thrusting to strike-slip faulting. *Geodinamica Acta 14(1–3),* 177–195.

Konno, K., Ohmachi, T. 1998. Ground-motion characteristics estimated from spectral ratio between horizontal and vertical components of microtremor. *Bulletin of the Seismological Society of America 88(1),* 228–241.

Kramer, S.L. 1996. *Geotechnical Earthquake Engineering Upper Saddle River*. NJ: Prentice Hall, 653 pp.

Lermo, J., Chávez-García, F.J. 1994a. Are microtremors useful in site response evaluation? *Bulletin of the seismological society of America 84(5),* 1350–1364.

Lermo, J., Chávez-García, F.J. 1994b. Site effect evaluation at Mexico City: dominant period and relative amplification from strong motion and microtremor records. *Soil Dynamics and Earthquake Engineering 13(6),* 413–423.

McKenzie, D. 1972. Active tectonics of the Mediterranean region. *Geophysical Journal International 30(2)* 109–185.

Mogi, K. 1962. Magnitude-Frequency Relationship for Elastic Shocks Accompanying Fractures of Various Materials and Some Related Problems in Earthquakes. *Bulletin of Earthquake Engineering, University of Tokyo* 40, 831–853.

Nakamura, Y.1989. A method for dynamic characteristics estimation of subsurface using microtremor on the ground surface. Railway Technical Research Institute. *Quarterly Reports 30(1),*25-33.

Nakamura, Y. 2019. What Is the Nakamura Method? *Seismological Research Letters 90*, 1437–1443.

Ogata, Y., Imoto, M., Katsura, K. 1991. 3-D spatial variation of b-values of magnitude-frequency distribution beneath the Kanto District, Japan. *Geophysical Journal International 104,*135–146.

Ormeni, R., Ozturk, S., Fundo, A., Celik, K. 2017. Spatial and temporal analysis of recent seismicity in different parts of the Vlora-Lushnja-Elbasani-DibraTransversal Fault Zone, Albania. *Austrian Journal of Earth Sciences 110(2),* 1-17.

Ozer, C., Ozyazicioglu, M., Perk, S. 2022a. Coda Wave Spatial Variation in Eastern Anatolia, Turkey. *Journal of Brilliant Engineering 2*, 4639.

Ozer, C., Ozturk, S., Pamuk, E. 2022b. Tectonic and structural characteristics of Erzurum and its surroundings (Eastern Turkey): a detailed comparison between different geophysical parameters. *Turkish Journal of Earth Sciences 31(1),* 85–108.

Ozturk, S. 2013. A statistical assessment of current seismic quiescence on the North Anatolian Fault Zone: Earthquake precursors. *Austrian Journal of Earth Sciences 106(2)*, 4–17.

Ozturk, S. 2017. Space-time assessing of the earthquake potential in recent years in the Eastern Anatolia region of Turkey. *Earth Sciences Research Journal 21(2),* 67–75.

Ozturk, S., Cinar, H., Bayrak, Y., Karsli, H., Daniel, G. 2008. Properties of the aftershock sequences of the 2003 Bingol, MD = 6.4, (Turkey) earthquake. *Pure and Applied Geophysics 165(2)*, 349–371.

Pamuk, E., Fırat, S., Büyüksaraç, A., Çetin, K.Ö., Bek-

taş, Ö., Işık, N.S., Sarıtepe, H.E. 2026. Three dimensional shear wave velocity (Vs) structure and dynamic soil properties of Adıyaman-Gölbaşı basin using HVSR and SPAC methods. *Soil Dynamics and Earthquake Engineering 200*, 109744.

Reasenberg, P. 1985. Second-order moment of central California seismicity, 1969–1982. *Journal of Geophysical Research: Solid Earth 90(B7),* 5479–5495.

Reilinger, R., McClusky, S., Oral, M., King, R., Toksoz, M., Barka, A., Kinik, I., Lenk, O., Sanli, I. 1997. Global Positioning System measurements of present-day crustal movements in the Arabia–Africa–Eurasia plate collision zone. *Journal of Geophysical Research: Solid Earth 102(B5)*, 9983–9999.

Sarac, B., Ozer, C. 2024. Soil dynamic features of Ataturk University Campus (Erzurum), eastern Türkiye, by microtremor method. *Baltica 37(2)*, 125-136.

Sengor, A. 1979. The North Anatolian transform fault: its age, offset and tectonic significance. *Journal of the Geological Society 136(3),* 269–282.

Sengor, A.C., Natal'InB, A. 1996. Turkic-type orogeny and its role in the making of the continental crust. *Annual Review of Earth and Planetary Sciences 24(1),* 263–337.

Sengor, A., Tuysuz, O., Imren, C., Sakinc, M., Eyidogan, H., Gorur, N., Le Pichon, X., Rangin, C. 2005. The North Anatolian fault: A new look. *Annual Review Earth Planetary Science 33*, 37–112.

Taymaz, T., Jackson J., McKenzie D. 1991. Active tectonics of the north and central Aegean Sea. *Geophysical Journal International 106(2),* 433–490.

Toksoz, M.N., Johnston, D.H., Timur, A. 1981. Attenuation of Seismic Waves in Dry and Saturated Rocks. In: *Seismic Wave Attenuation* (p. 105). Society of Exploration Geophysicists.

Yarbasi, N., Kalkan, E. 2009. Geotechnical mapping for alluvial fan deposits controlled by active faults: a case study in the Erzurum, NE Turkey. *Environmental Geology 58(4)*, 701–714.

Wathelet, M., Chatelain, J.L., Cornou, C., Giulio, G.D., Guillier, B., Ohrnberger, M., Savvaidis, A. 2020. Geopsy: A user-friendly open-source tool set for ambient vibration processing. *Seismological Research Letters 91(3),* 1878–1889.

Wiemer, S. 2001. A software package to analyze seismicity: ZMAP. *Seismological Research Letters 72(3),* 373–382.

Whitney, D.L., Delph, J.R., Thomson, S.N., Beck, S.L., Brocard, G.Y., Cosca, M.A., Umhoefer, P.J. 2023. Breaking plates: Creation of the East Anatolian fault, the Anatolian plate, and a tectonic escape system. *Geology 51(7),* 673–677.

Internet sources

Akbas, B., Akdeniz, N., Aksay, A., Altun, I., Balci, V., Bilginer E., *et al*. 2011. 1:1,250,000 scale Geological Map of Turkey. *Publication of General Directorate of Mineral Research and Exploration*. Ankara-Türkiye. http://yerbilimleri.mta.gov.tr (In Turkish).

Esri, USGS, NOAA. 2025. ArcGIS Online Basemap Service. Esri. Retrieved from https://www.esri.com

URL-1. http://www.koeri.boun.edu.tr/sismo/zeqdb/. Accessed Data: 01 January 2021.